

**$^{52}\text{Cr}$  Spinor Condensate: A Biaxial or Uniaxial Spin Nematic**

Roberto B. Diener and Tin-Lun Ho

*Department of Physics, The Ohio State University, Columbus, Ohio, USA*

(Received 30 November 2005; published 16 May 2006)

We show that the newly discovered  $^{52}\text{Cr}$  Bose condensate in zero magnetic field can be a spin nematic of the following kind: a “maximum” polar state, a “colinear” polar state, or a biaxial nematic ferromagnetic state. We also present the phase diagram with a magnetic field in the interaction subspace containing the chromium condensate. It contains many uniaxial and biaxial spin nematic phases, which often but not always break time reversal symmetry, and can exist with or without spontaneous magnetization.

DOI: [10.1103/PhysRevLett.96.190405](https://doi.org/10.1103/PhysRevLett.96.190405)

PACS numbers: 03.75.Mn

Recently, Tilman Pfau’s group at Stuttgart has succeeded in condensing a Bose gas of  $^{52}\text{Cr}$  atoms [1]. These are spin-3 bosons with electronic spin  $J = 3$  and nuclear spin  $I = 0$ . In contrast, alkali-metal bosons such as  $^{87}\text{Rb}$  and  $^{23}\text{Na}$  are spin-1 or -2 bosons with  $J = 1/2$  and  $I = 3/2$ . Since  $^{52}\text{Cr}$  atoms have a value of  $J$  which is 6 times larger than that of the alkali metals, their dipolar interaction constant is 36 times larger. Indeed, dipolar effects have been observed in the expansion of polarized Cr condensates [2], although they have not yet been observed in the alkali metals. For this reason, Cr is sometimes referred to as a “dipolar condensate,” although this characterization is not quite appropriate since the dipolar energy is no more than a few percent of the total energy. As we shall see, if the spin degree of freedom of Cr is released, it will show many remarkable spin nematic structures stabilized by energies much larger than the dipolar energy. The Cr condensate, in short, is a quantum spin nematic.

At present, experiments on  $^{52}\text{Cr}$  are performed in magnetic traps which freeze the atomic spins. The spin degrees of freedom, however, can be released in optical traps. In the case of optically trapped  $^{87}\text{Rb}$  and  $^{23}\text{Na}$ , ground states of different magnetic structures have been discovered. Since Cr atoms have a higher spin, the number of possible phases will increase. Cr condensate also differs from the alkali metals in that its scattering lengths in different angular momentum channels are very different, whereas they are very similar in the alkali metals [3–5]. According to Ref. [4], the closer these scattering lengths, the weaker the spin-dependent interactions. Thus the ratio between spin-dependent and density-density interactions in the alkali metals is about 1% while it is of order 1 in  $^{52}\text{Cr}$ . In other words, once the spins of Cr are unfrozen, *the spin-dependent interactions overwhelm the dipolar energy*. Any novel properties of Cr spinor Bose-Einstein condensates (BECs) will be consequences of the spin interaction with dipolar effects as a perturbation.

For spin-3 bosons, the interactions are specified by the scattering lengths  $a_S$  for collisions with a total angular momentum  $S = 0, 2, 4, 6$ . All  $a_S$  except the one for  $S = 0$  have been determined experimentally [2]. The physical

system therefore lies on a line in the interaction parameter space, which we refer to as the “Cr” line. While we shall focus on this line, we also present the phase diagram as a function of the interaction constants  $\{a_S\}$  and magnetic field, for it will be useful for other spin-3 Bose systems. As we shall see, the phase diagram is full of spin nematic phases which are either uniaxial or biaxial. These phases typically but not always break time reversal symmetry, which can come about with and without a spontaneous magnetization [6,7]. The discovery of some of these nematic phases will be exciting indeed.

*The spin-dependent energy functional.*—Let  $\Psi_m = \sqrt{n}\zeta_m$ ,  $m = -3$  to 3, be the condensate wave function of a spin-3 Bose gas, where  $n$  is the density, and  $\zeta^\dagger\zeta = 1$ . As shown in Ref. [4], the ground state of a homogenous or single mode spinor condensate in zero magnetic field is determined by the energy  $E/E_o = \sum_{S=0,2,4,6}\tilde{a}_S\mathcal{P}_S$ ,  $\tilde{a}_S = a_S/a_B$ , where  $E_o = \int d^3r(2\pi\hbar^2 a_B/M)n^2$ ,  $a_B$  is the Bohr radius,  $\mathcal{P}_S = \sum_{M=-S}^S |B_{S,M}|^2$ , and  $B_{S,M} = \sum_{m,m'} \zeta_m^* \zeta_{m'} \langle S, M | 3, m; 3, m' \rangle$  is the amplitude of forming a boson pair in state  $|S, M\rangle$ . In the case of spin-1 alkali-metal gases (where  $S = 0, 2$  in the energy  $E$ ), the  $a_S$ ’s differ from each other only by about a few percent, so  $E$  is almost an identity. In contrast,  $^{52}\text{Cr}$  has  $a_2 = -7a_B$ ,  $a_4 = 58a_B$ ,  $a_6 = 112a_B$ , while  $a_0$  is undermined [2]. Using the method in Ref. [4],  $E$  can be written as [8]

$$E = E_o \left[ \alpha |\Theta|^2 + \beta \sum_{M=-2}^2 |B_M|^2 + \gamma \langle \mathbf{S} \rangle \cdot \langle \mathbf{S} \rangle + C \right], \quad (1)$$

where  $\langle \mathbf{S} \rangle = \zeta_m^* \mathbf{S}_{mm'} \zeta_{m'}$ ,  $B_M = \sqrt{7} B_{2,M}$ ,  $\Theta = \sqrt{7} B_{0,0}$ , so that  $\mathcal{P}_2 = 7 \sum_M |B_M|^2$ . The coefficients are defined as  $\alpha = \frac{1}{7a_B} [(a_0 - a_6) + \frac{21}{11}(a_6 - a_4)]$ ,  $\beta = \frac{1}{7a_B} [(a_2 - a_6) + \frac{18}{11}(a_6 - a_4)]$ ,  $\gamma = \frac{1}{11a_B}(a_6 - a_4)$ , and  $C = \frac{1}{7a_B} [a_6 - \frac{9}{11}(a_6 - a_4)]$ . We then have  $\beta = -4.38$ ,  $\gamma = 4.91$ ,  $C = 9.69$ , and  $\alpha$  undetermined. Using the relation between  $\mathbf{S}_1 \cdot \mathbf{S}_2$ ,  $(\mathbf{S}_1 \cdot \mathbf{S}_2)^2$  and the projection operators  $P_i$  [9], we can further express Eq. (1) in terms of the nematic tensor  $\mathcal{N}_{ij} \equiv \langle (S_i S_j + S_j S_i) \rangle / 2$  as

$$E/E_o = \bar{\alpha} |\Theta|^2 + \bar{\beta} \text{Tr } \mathcal{N}^2 + \bar{\gamma} \langle \mathbf{S} \rangle \cdot \langle \mathbf{S} \rangle + \bar{C}, \quad (2)$$

where  $\bar{\alpha} = \alpha - \frac{5}{3}\beta$ ,  $\bar{\beta} = \beta/18$ ,  $\bar{\gamma} = \gamma - \frac{5}{12}\beta$ ,  $\bar{C} = C - \beta$ . For Cr, we have  $\bar{\beta} = -0.243$ ,  $\bar{\gamma} = 6.74$ ,  $\bar{C} = 14.1$ , and  $\bar{\alpha}$  is unknown.

*Dipolar energy.*—To get an idea of the general structure of  $E_D$ , we use the single mode approximation so that all components of  $\Psi_\mu$  have the same spatial dependence  $\Psi_\mu(\mathbf{r}) = \sqrt{n(\mathbf{r})}\zeta_\mu$ , and  $\zeta_\mu$  is fixed. For harmonic traps  $V_T = \frac{M}{2} \sum_{i=1}^3 \omega_i^2(\mathbf{r} \cdot \hat{\mathbf{a}}_i)^2$ , where  $(\hat{\mathbf{a}}_1, \hat{\mathbf{a}}_2, \hat{\mathbf{a}}_3)$  is an orthonormal triad, the dipole energy is [see footnote [10]]

$$E_D/E_o = \sum_{i=1}^3 \eta_i [\langle \mathbf{S} \rangle \cdot \hat{\mathbf{a}}_i]^2, \quad (3)$$

where  $\eta_i = \frac{1}{2E_o}(g\mu_B)^2 \int d\mathbf{r}_1 d\mathbf{r}_2 n(\mathbf{r}_1)n(\mathbf{r}_2)[1 - 3(\hat{\mathbf{a}}_i \cdot \hat{\mathbf{r}})^2]/r^3$ ,  $\mathbf{r} = \mathbf{r}_1 - \mathbf{r}_2$ . In particular, we denote the direction with smallest  $\eta$  as  $\hat{\mathbf{a}}_3$ . Combining the  $\gamma$  term in Eq. (1) with Eq. (3), all  $\langle \mathbf{S} \rangle$ -dependent terms in the energy can be written as in Eq. (3) with  $\eta_i \rightarrow \eta_i + \gamma$ . The effect of the dipole energy is to align  $\langle \mathbf{S} \rangle$  along the direction  $\hat{\mathbf{a}}_3$ . The phase diagram in zero magnetic field including dipole energy can therefore be obtained by first minimizing Eq. (1) (without dipole energy), then replacing  $\gamma$  by  $\gamma - \eta_3$ , and aligning the spontaneous magnetization of those phases that acquire it along  $\hat{\mathbf{a}}_3$ .

To estimate the magnitude of  $\eta_i$ , it is straightforward to show that  $\eta_i = \frac{-(g\mu_B)^2}{4\pi\hbar^2 a_B/M} \frac{4\pi I_i}{3} = -1.7I_i$  where  $I_i = \int_{\mathbf{q}} |n(\mathbf{q})|^2 [1 - 3(\hat{\mathbf{a}}_i \cdot \hat{\mathbf{q}})^2] / \int_{\mathbf{q}} |n(\mathbf{q})|^2$ . Approximating  $n(\mathbf{r})$  as a Gaussian so that  $n(\mathbf{q}) = C e^{-\sum_{i=1}^3 q_i^2 R_i^2}$ , where  $R_i$  is the radius of the atom cloud along  $\hat{\mathbf{a}}_i$  and assuming a cylindrical trap ( $R_x = R_y = R_\perp \neq R_z$ ),  $I_z$  varies from 0 to 1 as  $R_z/R_\perp$  varies from 1 to 10. Thus,  $\eta_i$  is at most about 25% of  $\gamma$ . As we shall see, all the phases along the Cr line either have zero magnetization, or a weak spontaneous magnetization such that the  $\gamma$  term in Eq. (1) contributes very little to the total energy. Since  $E_D$  is dominated by the  $\gamma$  term, it can be ignored as a first approximation.

*Relation between singlet amplitude  $\Theta$ , magnetization  $\langle \mathbf{S} \rangle$ , and the nematic tensor  $\mathcal{N}$ .*—The quantities  $\Theta$ ,  $\langle \mathbf{S} \rangle$ , and  $\mathcal{N}$  provide a characterization of the phases. They are, however, not independent quantities. Let us first consider  $\Theta$ , which is  $\Theta = 2\zeta_3\zeta_{-3} - 2\zeta_2\zeta_{-2} + 2\zeta_1\zeta_{-1} - \zeta_0^2 \equiv A_{mm'}^{(o)}\zeta_m\zeta_{m'}$ , where  $A_{mm'}^{(o)} = (-1)^{m+1}\delta_{m+m',0}$  is the matrix for spin change under time reversal. It is also easy to show that the maximum value of  $|\Theta|^2$  is 1, and the condition for this is that  $\zeta$  is invariant (up to a phase  $\chi$ ) under time reversal, i.e.,  $(A^{(o)}\zeta)_m^* = e^{i\chi}\zeta_m$ . This also implies  $\langle \mathbf{S} \rangle = 0$  [5]. Thus any state with  $|\Theta| < 1$  breaks time reversal symmetry.

In the presence of a magnetic field  $\mathbf{B} = B\hat{\mathbf{z}}$ , the rotational invariance of Eq. (1) implies that

$$E/E_o = \alpha|\Theta|^2 + \beta \sum_{M=-2}^2 |B_M|^2 + \gamma\langle \mathbf{S} \rangle^2 - p\langle S_z \rangle + C, \quad (4)$$

where  $p = g\mu_B B/E_o$ . Next, we note that the tensor  $\mathcal{N}$  is Hermitian. It then has the diagonal form  $\mathcal{N}_{ij} = \lambda_1 \hat{\mathbf{e}}_1 \hat{\mathbf{e}}_1 + \lambda_2 \hat{\mathbf{e}}_2 \hat{\mathbf{e}}_2 + \lambda_3 \hat{\mathbf{e}}_3 \hat{\mathbf{e}}_3$ , where  $\{\hat{\mathbf{e}}_a\}$  are the principal axes, ( $a = 1, 2, 3$ ),  $\hat{\mathbf{e}}_a \cdot \hat{\mathbf{e}}_b = \delta_{ab}$ , and the  $\lambda_a = \langle (\hat{\mathbf{e}}_a \cdot \mathbf{S})^2 \rangle > 0$  are the eigenvalues, satisfying

$$\lambda_1 + \lambda_2 + \lambda_3 = S(S+1) = 12, \quad S = 3. \quad (5)$$

We shall order the  $\lambda$ 's so that  $\lambda_1 \leq \lambda_2 \leq \lambda_3$ . The axes  $(\hat{\mathbf{e}}_1, \hat{\mathbf{e}}_2, \hat{\mathbf{e}}_3)$  will be referred to as minor, middle, and major axis, respectively. Without loss of generality, we can always arrange  $(\hat{\mathbf{e}}_1, \hat{\mathbf{e}}_2, \hat{\mathbf{e}}_3)$  in a right-handed triad. Using the terminology of liquid crystals, the system is referred as a (spin) nematic if  $\mathcal{N}$  is not isotropic, i.e., not proportional to the identity matrix. Systems with two identical eigenvalues and three unequal eigenvalues will be referred to as uniaxial and biaxial nematics, respectively.

The different phases arise from the competition of  $\Theta$ ,  $\langle \mathbf{S} \rangle$ , and  $\mathcal{N}$ , which are not independent quantities. Such competition can be illustrated by considering  $\bar{\beta} < 0$ , in which case  $\text{Tr } \mathcal{N}^2$  in Eq. (2) favors  $\lambda_3 = 9$ ,  $\lambda_1 = \lambda_2 = 3/2$ , which can be achieved by either the polar state  $(1, 0, 0, 0, 0, 0, 1)/\sqrt{2}$ , or the ferromagnetic state  $(1, 0, 0, 0, 0, 0, 0)$ . However, neither of these states are favored simultaneously by the  $\Theta$  term when  $\bar{\alpha} > 0$ , and the  $\langle \mathbf{S} \rangle^2$  term, since  $\bar{\gamma} > 0$  for Cr. One of the key features we find below is that magnetization (be it spontaneous or induced) is generally accompanied with biaxial nematicity. Even though the energy functional is rotationally symmetric about the external field  $\hat{\mathbf{z}}$ , this symmetry is broken spontaneously in the biaxial nematic state.

*IV. Phase diagram in zero magnetic field,  $p = 0$ .*—We have minimized Eq. (1) by a combination of analytic and numerical methods [11]. The phase diagrams are shown in Figs. 1 and 2. Since  $\alpha$  is unknown for  $^{52}\text{Cr}$ , the physical system lies on the dotted straight line (or Cr line for short) in Fig. 1,  $\beta/\gamma = -0.892$ . It passes through the phases A, B, and C, which we name ‘‘maximum polar’’ state (A),

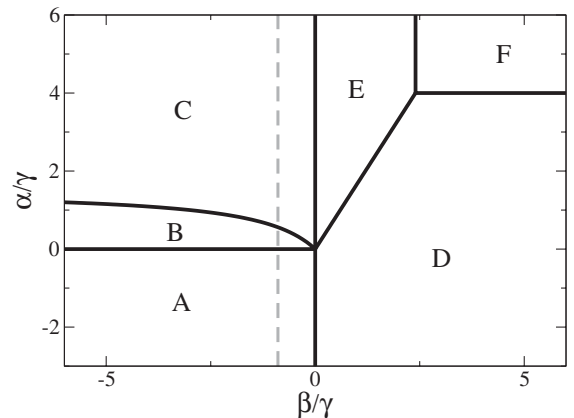


FIG. 1. Phase diagram in zero magnetic field for  $\gamma > 0$ . The dashed line (referred to as the Cr line) is where the physical system lies. The solid lines are first order boundaries. The nature of the phases displayed is discussed in Fig. 3.

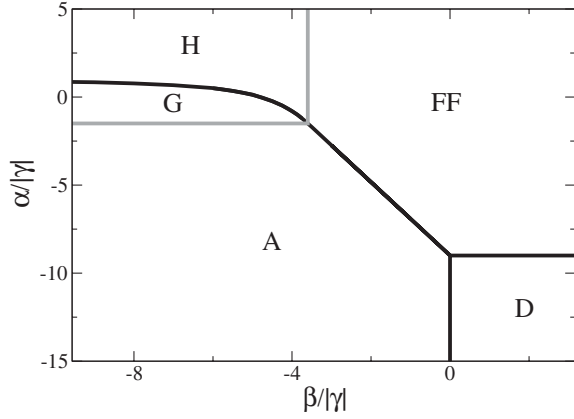


FIG. 2. Phase diagram in zero magnetic field for  $\gamma < 0$ . The solid and gray lines are first and second order boundaries, respectively. The nature of the phases is discussed in Fig. 3.

colinear polar state (*B*), and biaxial nematic ferromagnetic state (*C*), respectively. All order parameters  $\zeta$  displayed below are unique up to a phase factor and an arbitrary spin rotation.

*Symbols and notations.*—We characterize each phase by its condensate wave function  $\zeta$ , singlet amplitude  $\Theta$ , magnetization  $\langle \mathbf{S} \rangle$ , and nematic tensor  $\mathcal{N}$ . An isotropic  $\mathcal{N}$  ( $\lambda_1 = \lambda_2 = \lambda_3$ ) will be denoted by a sphere. Uniaxial nematics with ( $\lambda_1 = \lambda_2 < \lambda_3$ ) and ( $\lambda_1 < \lambda_2 = \lambda_3$ ) are represented by a long and flat cylinder, with major and minor axis being the symmetry axis of the cylinder, respectively. Biaxial nematics with ( $\lambda_1 < \lambda_2 < \lambda_3$ ) are represented as a “brick” with edge lengths given by  $\lambda_a$ . The principal axis  $\hat{\mathbf{e}}_a$  is parallel to the edge with length  $\lambda_a$ . Figure 3 shows the structure of the phases. In particular, (A) *Maximum polar state*: this state has time reversal symmetry, since  $\Theta = 1$ . It is a uniaxial nematic with  $\lambda_3 = 9$ ,  $\lambda_{1,2} = 3/2$ . (B) *Colinear polar state*: it is a superposition of two polar states  $(1, 0, 0, 0, 0, 1)$  and  $(0, 0, 1, 0, 1, 0, 0)$  with unequal weight and a relative phase.

Phase	$\langle \mathbf{S} \rangle$	Nematic tensor	$\Theta$	$\zeta$
A	0		1	$(1, 0, 0, 0, 0, 1)/\sqrt{2}$
B	0		$0 < \Theta < 1$	$(a, 0, be^{i\delta}, 0, be^{i\delta}, a)$
C	$> 0$	 $\langle \mathbf{S} \rangle \parallel \mathbf{e}_{2,3}$	$0 < \Theta < 1$	$(a, 0, b, 0, c, d)$
D	0		0	$(\sqrt{2}, 0, 0, i\sqrt{5}, 0, 0, \sqrt{2})/3$
E	0		$0 < \Theta < 1$	$(a, 0, b, 0, c, d)$
F	2		0	$(0, 1, 0, 0, 0, 0, 0)$
FF	3	 $\langle \mathbf{S} \rangle \parallel \mathbf{e}_3$	0	$(1, 0, 0, 0, 0, 0, 0)$
G	$> 0$	 $\langle \mathbf{S} \rangle \parallel \mathbf{e}_1$	$0 < \Theta < 1$	$(0, a, 0, b, 0, c, 0)$
H	$> 0$	 $\langle \mathbf{S} \rangle \parallel \mathbf{e}_3$	0	$(a, 0, 0, 0, 0, b, 0)$

FIG. 3. Phases present at  $p = 0$ .  $a, b, c, d$ , and  $\delta$  are real numbers.

This system is nonmagnetic  $\langle \mathbf{S} \rangle = 0$  and yet has broken time reversal symmetry,  $0 < |\Theta| < 1$ . The latter is achieved by the phase angle  $\delta$ , which varies from 1.3 to 1.4 along the Cr line from bottom to top. The system is uniaxial nematic with  $\lambda_1 < \lambda_2 = \lambda_3$ . (C) *Biaxial nematic ferromagnet*: the system has a weak *spontaneous magnetization*  $\langle \mathbf{S} \rangle = M\hat{\mathbf{z}}$ ,  $M = 0.07$  to  $0.08$ , and is a biaxial nematic with either  $\hat{\mathbf{e}}_2$  or  $\hat{\mathbf{e}}_3$  along  $\langle \mathbf{S} \rangle$ . Since  $M$  is small, the contribution of the  $\gamma$  term in Eq. (1) (and hence dipolar energy) is a very small contribution to the total energy. This structure is driven largely by the competition between the nematic and the singlet contributions. The boundary separating *B* and *C* is  $\tilde{\alpha} = 3|\tilde{\beta}|/(3|\tilde{\beta}| + 2)$ ,  $\tilde{\alpha} = \alpha/\gamma$ ,  $\tilde{\beta} = \beta/\gamma$ . The behavior of  $\lambda_a$  and  $|\langle \mathbf{S} \rangle|$  is shown in Fig. 4. The properties of these phases are tabulated in Fig. 4. The boundary between *G* and *H* is  $\tilde{\alpha} = (24\tilde{\beta} + 5\tilde{\beta}^2)/(36 + 24\tilde{\beta} + 5\tilde{\beta}^2)$  [12].

*Phase diagram in nonzero magnetic field.*—Figure 5 shows the phase diagram along the Cr line in Fig. 1 for  $p \neq 0$  obtained by minimizing Eq. (4). It has an intricate structure near  $\alpha = 0$ . All states have nonzero magnetization  $\langle \mathbf{S} \rangle$  along the direction of the magnetic field  $\hat{\mathbf{z}}$ , represented as an arrow. The main features of our results are:

- (i) The transition  $A_1 \rightarrow Z_1 \rightarrow G_1$  is a rotation of the uniaxial nematic tensor in the  $A_1$  phase (represented as a long cylinder) along its middle principal axis  $\hat{\mathbf{e}}_2$  as one crosses the phase  $Z_1$ , with the rotation angle finally reaching  $90^\circ$  at the  $G_1$  phase. However, in the  $Z_1$  phase,  $\mathcal{N}$  acquires biaxial nematicity, which continues into the  $G_1$  phase.
- (ii) As  $p \rightarrow 0$ , for  $\alpha/\gamma < -0.372$  and  $\alpha/\gamma > -0.372$ , the states  $\zeta_{A_1}^T$  and  $\zeta_{G_1}^T$  reduce to  $(1, 0, 0, 0, 0, 1)/\sqrt{2}$  and  $(0, \sqrt{3}, 0, \sqrt{10}, 0, \sqrt{3}, 0)/4$ , respectively, which are related to each other by a  $90^\circ$  rotation about  $\hat{\mathbf{y}}$ .
- (iii) The transition  $A_1 \rightarrow Z_1 \rightarrow H_1$  is a similar rotation process as in (i) except that the rotational angle is zero when one reaches the  $H_1$  phase. The nematic tensor  $\mathcal{N}$  of  $H_1$  is again uniaxial, except that  $H_1$  has zero singlet amplitude, unlike  $A_1$ .
- (iv)  $G_1$  and  $G_2$  have similar tensor  $\mathcal{N}$ . There is, however, a jump in  $\Theta$  across their boundary.
- (v) As the *B* phase in Fig. 1 extends into the  $B_1$  phase in

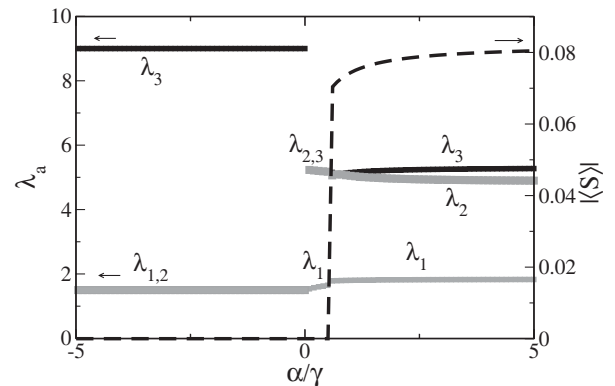


FIG. 4. The eigenvalues  $\lambda_a$  of  $\mathcal{N}$  and the magnetization  $\langle \mathbf{S} \rangle$  along the Cr line in Fig. 1.

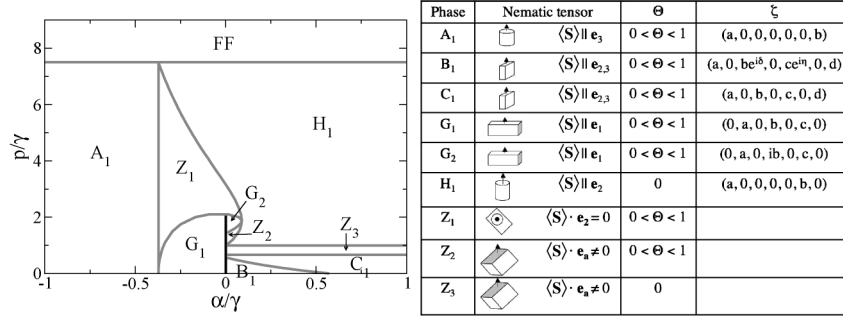


FIG. 5. Left panel: phase diagram for nonzero magnetic field along the Cr line in Fig. 1. The solid and gray lines are first and second order boundaries, respectively. Right panel: explanation of the phases in the diagram. The numbers  $a, b, c, d$  are real. All entries of the wave functions for the  $Z_j$  phases are generally nonzero. It is not clear they can be represented in a simple form as the other phases.

finite field  $p$ , its nematic tensor  $\mathcal{N}$  changes from uniaxial to biaxial, merging into the  $C_1$  phase, the finite field extension of  $C$ . (vi) Among all phases in finite field,  $Z_1, Z_2$ , and  $Z_3$  are the ones where none of their principal axes are aligned with  $\hat{z}$ . The  $Z_1$  has its middle axis  $\hat{e}_2 \perp \hat{z}$ . In both  $Z_2$  and  $Z_3$ , none of the direction cosines  $\hat{e}_a \cdot \hat{z}$  vanish. Among these three phases,  $Z_3$  is the only phase that has vanishing singlet amplitude. The phase boundary between  $C_1 - Z_3$  and  $Z_3 - H_1$  are straight lines at  $p/\gamma = 0.667$  and  $1$ , respectively. (vii) The system becomes a full ferromagnet ( $FF$ ) when  $p/\gamma > 7.5$ . To observe the spinor feature, we then need  $B < B_c$ , where  $B_c = (7.5)\gamma(2\pi\hbar^2 a_B n/M)/(g\mu_B)$ . Using  $g = 2$ ,  $\gamma = 4.91$ , we have  $B_c = [8.34 \times 10^{-19} n]$  Gauss, where  $n$  is in units of  $\text{cm}^{-3}$ . Thus, with  $n = 5 \times 10^{12}$  to  $10^{14} \text{ cm}^{-3}$ ,  $B_c = 4.2 \times 10^{-6}$  to  $10^{-4}$  Gauss.

**Detection.**—Although the ground states of Eq. (1) are determined up to an arbitrary rotation about  $\hat{z}$ , this degeneracy can be lifted by the anisotropy of a trap through dipole interaction Eq. (3). With the principal axes (i.e.,  $\{\hat{e}_a\}$ ) fixed by the magnetic field and the trap, the eigenvalues  $\lambda_a$  can be determined by performing Stern-Gerlach experiments along the axes  $\hat{e}_a$ .

**Final remarks.**—The realization of quantum spin nematics, especially the biaxial ones, will be an exciting development in both cold atom and condensed matter physics. These novel states are yet to be realized in solid state systems, and biaxial nematics are known to have non-Abelian defects. Although reducing the magnetic field to the spinor regime for Cr is a challenging task, screening a field to  $10^{-4}$  Gauss is not outside the reach of current technology. From the present work, we expect spin nematics will also be found in other higher spin Bose gases.

T. L. Ho would like to thank T. Pfau and Marco Fattori for discussions. This work is supported by NASA Grant No. NAG8-1765 and NSF Grant No. DMR-0426149.

- [1] A. Griesmaier *et al.*, Phys. Rev. Lett. **94**, 160401 (2005).
- [2] J. Stuhler *et al.*, Phys. Rev. Lett. **95**, 150406 (2005).
- [3] Since the spins of  $^{52}\text{Cr}$  bosons are electronic, they interact with *electronic* singlet and triplet potentials, which typically give rise to very different scattering lengths. In contrast,  $F = 1$  and  $F = 2$  alkali-metal bosons carry hyperfine spins. The differences between scattering lengths in these states are much smaller than those for electronic spins.
- [4] T. L. Ho, Phys. Rev. Lett. **81**, 742 (1998).
- [5] C. V. Ciobanu *et al.*, Phys. Rev. A **61**, 033607 (2000).
- [6] Biaxial nematics do not exist in zero field in  $F = 1$  and  $F = 2$  Bose gases. For spin-3 Bosons like Cr, it can exist even in zero field ( $C$  phase in Fig. 1).
- [7] Recently, Santos and Pfau [this issue, Phys. Rev. Lett. **96**, 190404 (2006)] have studied the same problem. They obtain a phase diagram qualitatively similar to ours. They do not distinguish the  $B$  and  $G$  phases (between which we find a first order phase transition). Their view is that these phases are practically degenerate, making it hard to differentiate experimentally. They also neglect our  $Z$  phases, which are close in energy with other phases.
- [8] Using the identities  $1 = P_0 + P_2 + P_4 + P_6$ ,  $\mathbf{S}_1 \cdot \mathbf{S}_2 = -12P_0 - 9P_2 - 2P_4 + 9P_6 = 9 - 21P_0 - 18P_2 - 11P_4$  for a pair of spin-3 bosons with contact interaction, where  $P_S$  is the projection operator for total spin  $S$ , we can trade  $P_6$  and  $P_4$  with a constant and  $\mathbf{S}_1 \cdot \mathbf{S}_2$ .
- [9] Using  $(\mathbf{S}_1 \cdot \mathbf{S}_2)^2 = 81 + 63P_0 - 77P_4 = 18 + 210P_0 + 126P_2 + 7\mathbf{S}_1 \cdot \mathbf{S}_2$ , we have  $\sum_M |B_M|^2 = \frac{1}{18} \text{Tr } \mathcal{N}^2 - \frac{5}{12} \times \langle S \rangle^2 - \frac{5}{3} |\Theta|^2 - 1$ .
- [10]  $E_D = \frac{(g\mu_B)^2}{2} \int d\mathbf{r} d\mathbf{r}' n(\mathbf{r})n(\mathbf{r}') \langle S_i \rangle_r \langle S_j \rangle_{r'} D_{ij}(\mathbf{r} - \mathbf{r}')$ , where  $g$  is the Landé  $g$  factor,  $\mu_B$  is the Bohr magneton,  $D_{ij}(\mathbf{R}) = (\delta_{ij}R^2 - 3R_i R_j)/R^5$ , and  $\langle S \rangle_r = \zeta_\mu^z(\mathbf{r}) \mathbf{S}_{\mu\nu} \zeta_\nu(\mathbf{r})$ .
- [11] Phase transitions are found by looking for discontinuities of derivatives of the ground state energy as a function of the parameters in the Hamiltonian.
- [12] For  $\beta/|\gamma| < -6$  the  $H$  phase is degenerate with the  $I$  phase, which is a uniaxial nematic with  $\langle S \rangle \parallel e_1$ .